Biofilm Removal Efficacy Using Direct Electric Current in Cross-Flow Ultrafiltration Processes for Water Treatment

Sarah Kerdi, Adnan Qamar, Johannes S. Vrouwenvelder, Noreddine Ghaffour

King Abdullah University of Science and Technology (KAUST), Water Desalination and Reuse Center (WDRC), Biological and Environmental Science and Engineering (BESE), Thuwal 23955-6900, Saudi Arabia, Email: noreddine.ghaffour@kaust.edu.sa.

Abstract

Biofouling of membranes in water treatment is considered as one of the major practical problems. A novel and an efficient approach for cleaning biofilm grown on the membrane surface is proposed by applying a direct electric current (124 mA, 90 s) through platinum electrodes inside a cross-flow ultrafiltration channel. Depending on the electrochemical reactions occurring at the electrodes, either chlorine or hydrogen-producing configuration is realized by interchanging the current polarity. Baseline determination of the amount of chlorine generated and change in pH is assessed as a function of current intensity, linear cross-flow velocity, and duration of applied current. The efficiency of the proposed method is determined by investigating electrically treated biofilm through bacterial inactivation using Confocal Laser Scanning Microscopy (CLSM), bacterial cell structure changes through Scanning Electron Microscopy (SEM), and by estimating the amount of biomass removal through Optical Coherence Tomography (OCT). When a chlorine-producing electrode is placed at the inlet of the flow cell, 68% of bacterial inactivation is achieved without any modification of bacterial cell shape. Furthermore, a high and near-complete biomass removal is achieved (99%) after a subsequent forward flush of the electrically treated biofilm. However, placing a hydrogen-producing electrode at the inlet reveals a slightly lower bacterial inactivation (65%) and lower biomass removal (77%). Additional systematic experiments using individually sodium hydroxide (NaOH), sodium hypochlorite (NaOCl), or gas microbubbles enabled to elucidate the cause of biofilm removal, synergic effect of caustic agent NaOH and microbubbles.

Keywords: *Electrical Cleaning; Biofouling; Electrochemical; OCT; Filtration membranes.*

1. Introduction and background

Water filtration technologies primarily thrive on membrane processes as they have the potential to produce high quality of clean water at reasonable energy footprints. Biofilm growth on membrane surfaces during filtration presents a serious concern due to the quick proliferation of bacterial cells and the fast generation of extracellular polymeric substances (EPS) [1]. It tends to block the filtration channel, thereby significantly increasing the energy requirement of filtration processes. Thus, the biofouling prevention and removal from membrane surfaces remain a key challenge to improve membrane performance.

Several methods to control the development of biofouling on membrane surfaces are proposed in the past [2, 3]. Biological strategies, such as the use of bacteriophage [4], quorum sensors inhibitors [5, 6], addition of nitric oxide donors [7], water pretreatment [8-10] and bacteriostatic materials [11-16] aid in reducing bacterial attachment and biofouling. The optimization of hydrodynamic conditions by controlling the shear rate and flow turbulence has shown inherent biofouling mitigation by using unique feed spacers designs [17-22]. Besides, various physical processes are often utilized in industries to achieve membrane cleaning, such as hydraulic (backflushing, backwashing) [23], pneumatic (air bubbling, air sparging) [24, 25], and ultrasound [26-28] approaches. Contrary to physical treatments, the impact of chemical agents [29, 30] in the cleaning of membranes has been actively pursued [31, 32]. However, these traditional physical and chemical techniques have inherent drawbacks including lack of cleaning efficiency, high operating cost, production of toxic chemical by-products, damage/shorter lifespan of membranes, and limitations from industrial-scale applications [3, 33].

The use of an electric field through electrolysis process to effectively eliminate bacteria has been demonstrated in the past [34], mainly achieved due to cell lysis. Exemplary studies [35-39] have shown an effective or full microbial inactivation under varying experimental conditions (current intensity [35], duration of electrical shock [35, 37], electrode distance [37], bacteria type/concentration [36, 38, 39] and different electrolyte types [34]) when electrodes were directly placed in an electrolytic solution containing microbes. Wouters et al. [40] reported that electric treatment is more efficient in killing the bacteria than the heat inactivation. Under the direct application of current to the electrolytic solution, the bacterial inactivation is primarily achieved by the production of local disinfectant due to oxidation/reduction reactions taking place at electrodes and is further concomitant by a change in pH [37, 41].

Inspired by the active elimination of bacteria in an electrolytic suspension, attempts have been made to apply the electric field to mitigate biofouling developed on the membrane surface [36, 42-48]. Electro-kinetic methods (one electrode placed in the feed side and one electrode either located in the permeate side or represented by an electro-membrane) have shown the ability to remove the gel layer from the membrane through electrophoresis phenomena. These studies also demonstrated an enhancement in permeate water flux due to electroosmosis phenomenon, which occurs simultaneously and acts as an additional driving force for the feed stream [42, 49, 50]. In electro-kinetic methods, no local disinfectant, pH change, and microbubble formation occur as electrodes are separated by the membrane. The electrode presented in the feed side is exposed to the electrolytic solution, whereas the other electrode is in the permeate side (pure water or solvent), not allowing oxidation/reduction reactions at the electrodes. The use of alternating current by keeping both electrodes on the feed side has also been demonstrated [39, 44]. However, alternating current has a very low efficacy to produce electrochemical reactions [51]. Thus, cleaning with these methods [36, 42-45] only occurs due to the electrostatic repulsion mechanism, which is not very effective especially for pre-grown biofilm.

The biofilm removal using electro-conductive membrane [44, 51] and conductive feed spacer [45] is actively being studied. Electrically conductive surfaces like electro-conductive membranes or feed spacers, allow electrical current to pass through them. Mechanistically, this approach is slightly better compared to electro-kinetic methods. When current passes through the conductive surfaces, they not only act as electrostatic repulsion surfaces for oppositely charged bacteria but also trigger a small percentage of oxidation/reduction reactions (at the locations where electrodes are connected to membrane or spacer surface [51]). As most of the applied current passes through the membrane or feed spacer, usually no bubble formation occurs and a very small amount of disinfectant is generated. Thus, this approach performs slightly better than electro-kinetic methods.

From cleaning mechanism point of view, previous methods employed especially for membrane biofouling cleaning [36, 42-45] are not able to exploit full potential advantages offered by the application of electric field mainly; pH change, formation of disinfecting species and impact of gas bubbles (like seen when electrodes are submerged directly in electrolytic solution [34, 35]). In line with this idea, we study the efficacy of direct electric current on a biofilm (already grown on ultrafiltration (UF) membrane surface) removal/mitigation by simply introducing two electrodes at inlet and outlet (ensuring that electrodes are not in contact with membrane or spacer) of a cross-

flow cell [52]. Seawater is a natural electrolyte, converting flow-cell to an electrolytic cell in cross-flow conditions. Under the application of direct current [51] through inert electrodes made of platinum (Pt), electrochemical reactions (Eqs. 1-5) are induced and interact with already grown biofilm. The seawater electrolysis leads to the formation of chlorine and hydrogen gases at two electrodes associated with the generation of sodium hydroxide (NaOH) in the medium.

$$2Cl^- - 2\acute{e} \longrightarrow Cl_{2\,(g)} \qquad \text{(Anode)} \qquad (1)$$

$$Cl_{2\,(g)} + H_2O \longrightarrow HOCl + Cl^- + H^+ \qquad (2)$$

$$HOCl \rightleftharpoons OCl^- + H^+ \qquad (3)$$

$$2H_2O + 2\acute{e} \longrightarrow H_{2\,(g)} + 2OH^- \qquad \text{(Cathode)} \qquad (4)$$

$$Na^+_{(aq)} + OH^-_{(aq)} \longrightarrow NaOH_{(aq)} \qquad \text{(Medium)} \qquad (5)$$

The chlorine gas hydrolyzes in water to form hypochlorous acid (HOCl) and hypochlorite ions (ClO^-), which are recognized as the major oxidants for water disinfection. As bacteria are embedded in EPS matrix of the biofilm, the production of chlorine/hydrogen gas microbubbles through electrochemical reactions associated with other compounds (like NaOH, HOCl/OCl^-) helps in immediate inactivation and EPS degradation resulting in biofilm removal.

In the present work, we demonstrate our proposed patented technique [52] in a lab-scale setup using a cross-flow cell mimicking the feed side of an industrial-scale UF module. For the proposed technique, we do not anticipate any change in filtration performance as electrodes are not in contact with membrane or feed spacer like observed for electrophoresis/electroosmosis methods. Thus, for simplicity and to primarily focus on biofilm removal effectiveness, a non-pressurized and non-permeating cross-flow filtration cell equipped with a UF membrane along with the feed spacer is used in the present study. The impact of *in-situ* applied electric current on the membrane biofouling is first investigated. Subsequently, key parameters determining cleaning efficiency of biofilm from the membrane surface have been identified, demonstrating the validity of the proposed technology for efficient membrane cleaning, especially for seawater desalination.

2. Experimental section

2.1. Materials

Polyethersulfone (PES) UF membrane (Synder LY flat sheet membrane, model YMLY3001, molecular weight cut-off (MWCO) = 100 kDa, Synder Filtration, Vacaville, CA, USA) and a feed spacer [17] (volume of 690 mm^3) in-house prototyped by 3-D printer technology were used in this work. Platinum (Pt) electrodes (cylindrical wires, diameter 0.5 mm, total length 26.6 mm, total area 42.2 mm^2, purity 99.95%, Alfa Aesar, Haverhill, Massachusetts, USA) placed at inlet and outlet of the flow cell (not in contact with either membrane or feed spacer) were employed in order to trigger the electrolysis inside the flow cell. The length of Pt wires, which are specifically immersed in the flowing feed solution, is 12.6 mm with an area calculated of 20.2 mm^2. As platinum is chemically recognized as an inert element, it does not participate in the redox reactions. For electrical shock experiments, the bacterial feed suspension consisted of 2 g of Bacto™ Yeast Extract (Extract of Autolyzed yeast cells, Becton Dickinson and Company) dissolved in 0.5 L of natural Red Sea water and incubated at 30 ^{0}C for 24 h. The obtained suspension was further diluted by adding 1.5 L of seawater. The conductivity of the feed solution was measured to be 60.5 mS/cm.

2.2. Experimental lab-scale setup of electrical shock experiments

The experimental setup of electrical shock experiments in a cross-flow UF channel is illustrated in Figure 1. The base of the used flow cell channel was fully occupied by a membrane and feed spacer having dimensions of (85 mm x 19 mm) and a height of 1.2 mm. The prepared feed bacterial solution was pumped to the flow cell by a gear pump (Model 75211-70, Cole-Parmer) at a volumetric flow rate (Q) of 100 mL/min (corresponding to the inlet feed flow velocity of U_0 = 0.073 m/s) throughout the growth of biofilm (10 days). To test the attachment strength of the pre-grown biofilm on the membrane surface, a flushing process was carried out at day 11 of biofilm development by increasing five times the flow rate to reach 500 mL/min (U_0 = 0.365 m/s) for 30 s. Subsequently, a constant electrical shock (current intensity I = 124 mA and voltage E = 62 V) was applied in one step for a shock time (t) of 90 s on platinum electrodes, which were initially immersed within the flowing bacterial feed solution based seawater. The electrically shocked biofilm was characterized by Scanning Electron Microscopy (SEM) and Confocal Laser Scanning Microscopy (CLSM) (Section 2.3). For the experiments aiming to determine the biofilm removal efficiency of this approach, the electrical shock was followed by a flushing process at a volumetric

flow rate of 500 mL/min (U_0 = 0.365 m/s) for 30 s and the remained biofouling on membrane surface was monitored by Optical Coherence Tomography (OCT) (Section 2.3).

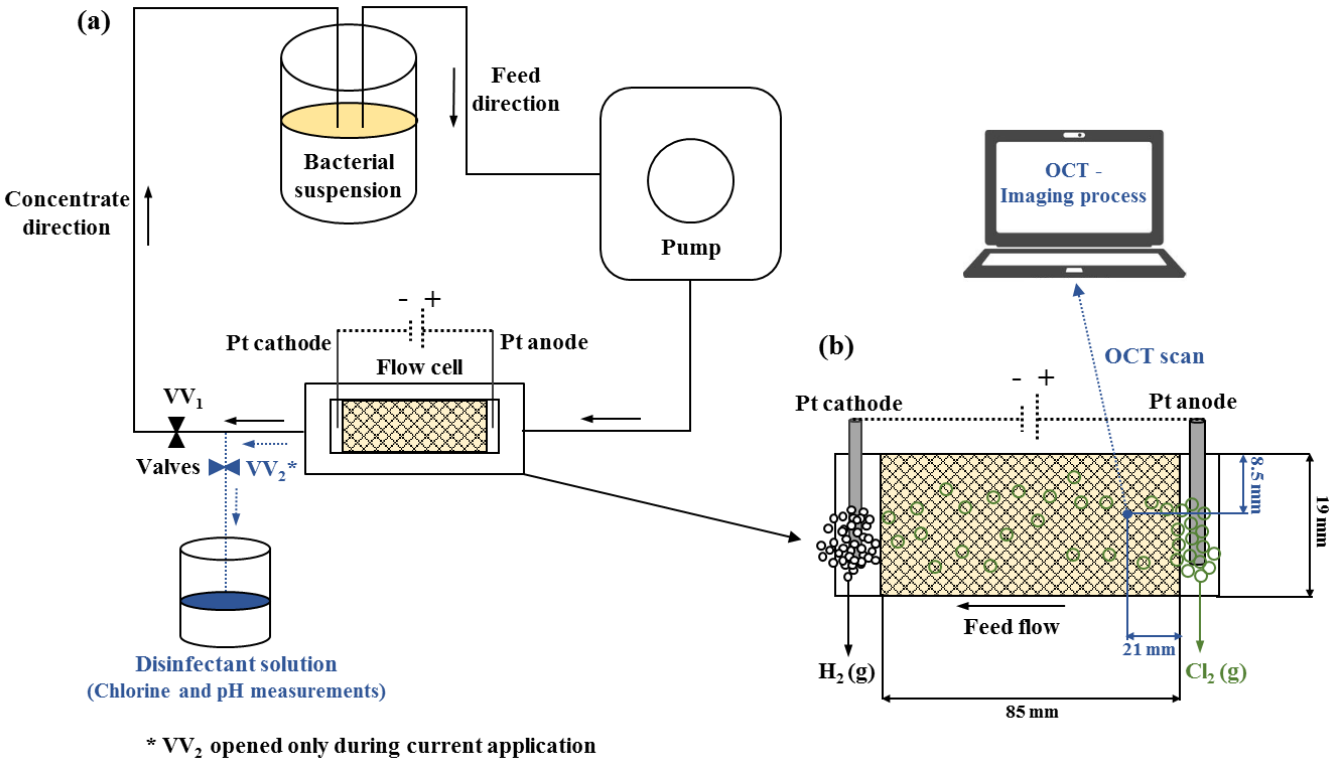

Figure 1. Schematic of the lab-scale setup of electrical shock experiments to evaluate biofilm treatment (a), and graphic illustrated the electrolysis process carried out in the flow cell unit in case of chlorine configuration along with dimensions of the utilized flow cell and OCT scanned location (blue dot shown in the flow cell) (b).

For the application of electric current, platinum electrodes were connected to a DC power supply (DC, BK Precision, Yorba Linda, CA, USA). They were placed at the input and output sides of the flow cell separated at a distance of 89.6 mm. Two configurations were investigated in this study: (a) chlorine configuration and (b) hydrogen configuration. When the anode (positive electrode) is placed at the inlet of the flow cell, it is referred to as chlorine configuration (chlorine microbubbles produced at the inlet). Whereas, placing cathode (negative electrode) at the inlet is referred to as hydrogen configuration (hydrogen microbubbles are generated at the inlet). Either configuration is achieved by switching the DC polarity on Pt electrodes. It is worth to mention

here that during the application of electric current, the concentrate solution was inhibited to go back to the feed solution tank via a closed valve (VV_1 shown in Figure 1). The treated disinfectant solution was then collected throughout electrolysis in a separate tank via an opened valve (VV_2 shown in Figure 1) placed in the line of concentrate solution.

2.3. Characterization of biofouling before and after electrical treatment

For each configuration and at each step of biofouling treatment, three-dimensional (3D) images of biomass were *in-situ* scanning by Optical Coherence Tomography (OCT, Thorlabs Hyperion, A-scan rate: 127 Hz, refractive index: 1.35, central wavelength: 930 nm). The same dimensions of scanned areas were maintained for all images presented in the manuscript. The surface of scanned regions was estimated to be 0.2303 mm^2 (0.49 mm × 0.47 mm) with a scan depth (x-z plane) of 1.13 mm and a resolution of 147 × 180 × 499 pixels. Furthermore, the same location of biofouled membrane in the flow cell was persistently scanned for both configurations. The scans were taken at a distance of 21 mm from the inlet and symmetrically at the center, 8.5 mm away from the top edge of the membrane area, as depicted in Figure 1b. This location is selectively characterized as the gas microbubbles, and the other chemical compounds generated by electrolysis are substantially flowing over it during the electrical shock application. It is relevant to highlight here that owing to OCT software and hardware constraints, taking several scans at different locations per experiment was not possible, as once the OCT probe is set, it could not be moved to avoid losing the exact imaging location. Thus, only one location could be scanned per each experiment to monitor accurately the change in biomass occurred at various stages of treatment. However, the experiments were triplicated for each configuration type to confirm the efficiency of the proposed cleaning technology. Thus, three OCT biofouling structural images were acquired for each stage of treatment per each configuration type and further processed by using *Avizo* software (Field Electron and Ion Company, Hillsboro, OR, USA) [53] to determine their corresponding biomass volumes. The percentages of biofilm removal were then calculated by taking into account the biomass volumes initially pre-grown on the membrane surface (V_0) and their corresponding volumes remaining on the membrane after electrical shock/flushing (V_f), following this equation: % biofilm removal = $(V_0 - V_f)\times 100/V_0$. The standard deviations were calculated for the percentages of biofilm removal obtained from these triplicated experiments.

Moreover, the biofouled membrane was characterized by Scanning Electron Microscopy (SEM, Magellan, FEI). Confocal Laser Scanning Microscopy (CLSM, LSM710 upright confocal microscope, Zeiss, Germany) was also utilized to visualize the live/dead cells of the biofouling samples scraped from the membrane by using a metal knife scarper. The samples (having each a volume of 1 mL) were stained with 2 µM of Syto®9 green-fluorescent nucleic acid (Syto 9, 5 mM solution in DMSO, Molecular Probes, Eugene, Oregon, USA) and 30 µM of Propidium Iodide (PI, 1.0 mg/mL solution in water, Molecular Probes, Eugene, Oregon, USA). These probes were visualized after excitation at wavelengths of 488 nm and 561 nm for Syto 9 and PI, respectively. For each characterized sample, a stained biofilm volume of 20 µL was transferred on a microscopic glass slide to be performed by CLSM imaging. The average percentages of live/dead cells were determined through processing a sequence of CLSM images (obtained from triplicated experiments of each configuration) by *ImageJ* software (U.S. National Institutes of Health, Maryland, USA).

3. Results and discussion

The cleaning efficiency of a pre-grown biofilm on UF membrane using DC is experimentally investigated. The influence of operating parameters on chlorine generation inside the flow cell was first evaluated without any biofilm presence. Further, two configurations (chlorine (Section 3.1) and hydrogen (Section 3.2)) are utilized to investigate the efficacy of this method on the pre-grown biofilm and quantitatively evaluate the biofilm removal potential. Finally, the mechanisms responsible for effective cleaning and uprooting of biofilm from the membrane surface are presented by performing a few sets of additional individual dosing experiments (using only base, chlorine species, or gas microbubbles) to elucidate the biofilm removal mechanism.

3.1. Chlorine configuration

3.1.1. Chlorine generation and pH change by electrolysis in absence of biofilm

The active chlorine content in water (or produced locally by electrolysis of seawater) is known to have a lethal impact on microorganisms [35, 54]. When DC is applied, the amount of chlorine generated should be enough to trigger the killing of bacteria, and its minimal efficient values are dependent on the microbial resistance (bacterial family [55] and biofilm thickness/morphology). Therefore, the variation of free and total chlorine generated with the increasing of current intensity

(I) and voltage magnitudes (E), inlet linear feed flow velocity (U_0), and the duration of electrical shock (t) was evaluated and shown in Figure 2, along with pH change in the medium (experimental protocol of chlorine and pH measurements are described in Section S1 of Supplementary material).

The chlorine amount exhibited a quasi-proportional increase with the increase of applied current intensity and voltage magnitude for electrical shock time of 90 s at a linear feed flow velocity of 0.073 m/s (Figure 2a). The concentration of free chlorine raised from 0.3 mg/L at 10 mA (E = 5 V) to reach 7 mg/L at 124 mA (E = 62 V). The total chlorine production also evolved at the same rate (≈ 23 times of increase) with the increase of current intensity from 10 mA to 124 mA, where the concentrations were estimated to be 0.6 mg/L and 14 mg/L, respectively. A reduction of chlorine amount was obtained with the increase of linear feed flow velocity in the filtration channel at applied DC of 40 mA (E = 20 V) for 90 s (Figure 2b). At a high velocity of 0.183 m/s, the electrochemical process produced 0.7 mg/L and 2.2 mg/L of free and total chlorine, respectively. The same behavior of chlorine amount was previously observed in a research study established by Nath et al. [56]. They reported augmentation of active chlorine with the current density and its reduction with the increase of flow rate when they investigated the use of novel perforated graphite/stainless steel electrodes for electric current in the drinking water application.

The chlorine generation is also found to be influenced by the electrical shock time (Figure 2c). It produced 1.1 mg/L and 2.6 mg/L of free and total chlorine in 15 seconds of electrolysis at I = 40 mA (E = 20 V) and U_0 = 0.073 m/s. Moreover, the rate of chlorine production is found to be higher at short shock time (below 45 s). The variation of chlorine quantity versus the electrical shock time has rarely been measured [55]. However, the relationship between the electrical shock time and the inactivation rate of bacteria in the presence of electrochemical disinfectants [57, 58] was found to significantly decrease the bacterial survival rate with the increase of applied current duration. The pH of the untreated bacterial solution was also measured and was found to be 7.4, whereas the pH values of shocked bacterial solutions were in the range between 8.0 and 8.4 for all tested parameters. This raise of pH is attributed to the formation of NaOH in the medium through electrolysis [36]. At this range of pH, the chlorine species (HOCl and OCl^-) having a bactericidal effect exist simultaneously in the medium [59].

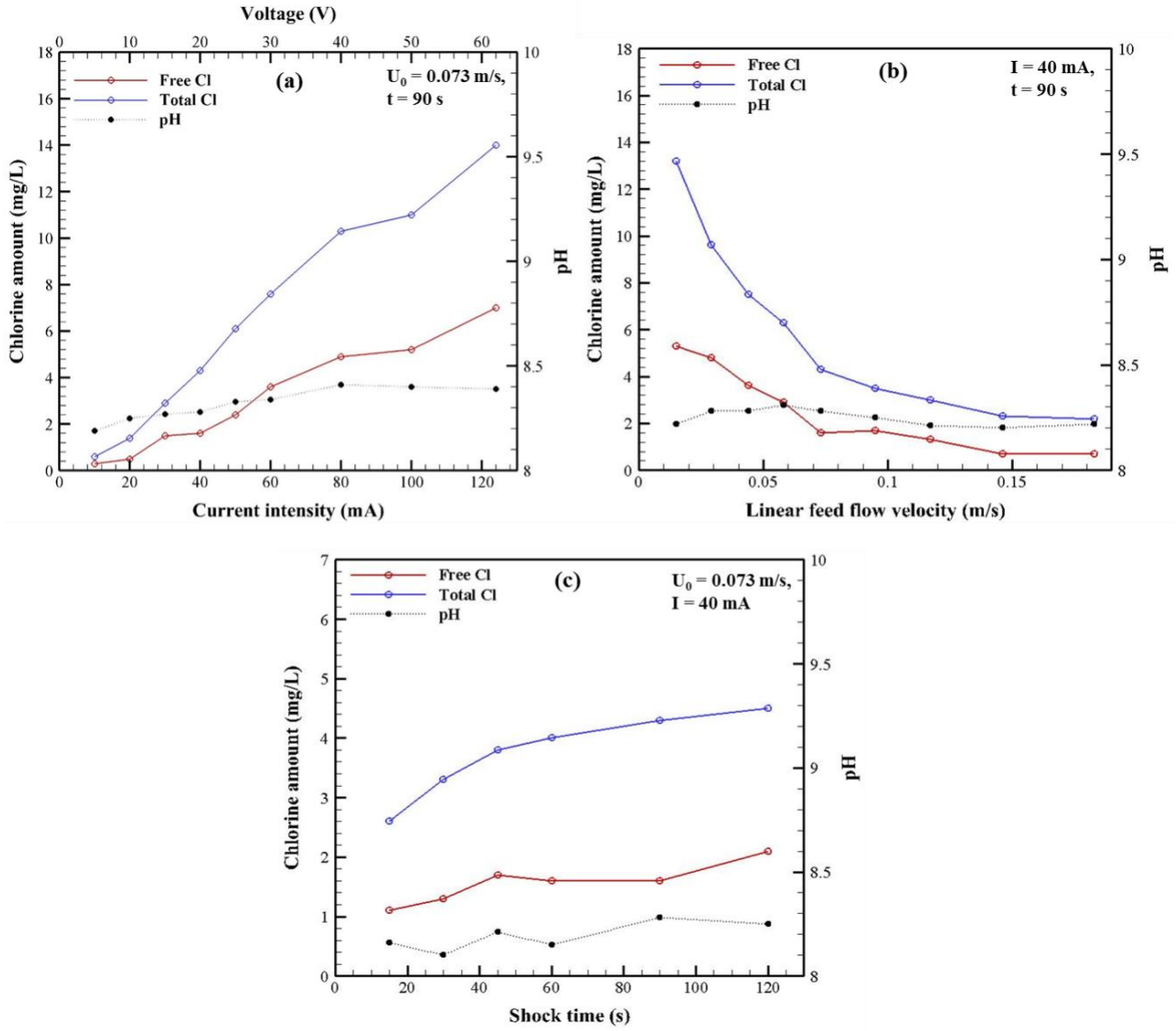

Figure 2. Quantity of free and total chlorine produced during the electrical treatment achieved in the flow cell in absence of biofilm, along with pH change in the medium, as a function of various parameters: Current intensity (a), inlet linear feed flow velocity (b), and electrical shock time (c). For (a), equivalent voltage magnitudes corresponding to the current intensities are as well plotted at the second X-axis.

In our experiments, the biofilm was developed over 10 days at slow linear velocity (U_0 = 0.073 m/s) to develop a thick, sticky and dense biofilm on the membrane surface [60]. This velocity was maintained during the application of DC on the pre-grown biofilm to avoid the interference of other factors on biofilm environment. Moreover, the electrical shock duration (t = 90 s) was selected based on the study of Ayoub et al. [37] who reported that for a low amperage (0.1 - 1 A), the electric treatment should be applied for a duration greater than 30 s in order to affect the bacterial cells. Once the linear velocity (U_0 = 0.073 m/s) and the shock time (t = 90 s) were figured out, these operating parameters were fixed to monitor the evolution of chlorine amount and pH as a function of current intensity increase (voltage amplitude increase), as plotted in Figure 2a. The generation of highest chlorine amounts (7 mg/L and 14 mg/L for free and total chlorine, respectively) along with the highest pH amplitude (pH = 8.4) in the medium at I = 124 mA (equivalent to E = 62 V) led to select this amperage/voltage magnitude for processing the electrical shock experiments on pre-grown biofilm.

3.1.2. Effect of electrical shock on a pre-grown biofilm

To investigate the bacterial inactivation capacity of the proposed technique, an electrically shocked biofilm was characterized by using CLSM. This electrically treated biofilm was compared with a sample of biofilm, which was not treated electrically. Figures 3a, b present the images of stained samples where the live and dead cells were shown in green and red colors, respectively. The analysis revealed that more live bacterial cells were visualized in case of unshocked biofoulant (Figure 3a) with average viability percentages estimated of 80% and 20% for live and dead cells, respectively (Table 1). Instead, for shocked biofouling, it displayed that 68% of bacterial cells were inactivated, and only 32% of them were survived (Figure 3b, Table 1). These results indicated that the killing of bacterial cells occurred within the biofilm matrix when a DC was applied inside the flow cell. Microbial inactivation in salt solution has been already investigated by directly applying electric current on the bacterial suspension [35, 37]. In our study, the bacteria are embedded within the biofilm and are not in direct contact with Pt electrodes where the current was applied (Figure 1). Hence, as a primary viewpoint, it was concluded that the inactivation of bacteria was not related to the current effect. The generation of chemical products (HOCl/ ClO^- and NaOH) in the medium could be solely responsible for the bacterial inactivation as they are recognized as bactericidal agents in previous studies [55, 58, 61, 62].

Table 1. Average viability percentages of bacterial cells for various unshocked and shocked biofoulant samples calculated based on confocal laser scanning microscopy images. For electrically treated biofouling sample in chlorine configuration, the amounts of free and total chlorine generated and passed over the biofilm are 7 mg/L and 14 mg/L, respectively.

Setup	Sample	Live cells (%)	Dead cells (%)
Chlorine configuration	Unshocked	80 ± 8	20 ± 8
	Electrical shocked	32 ± 4	68 ± 4
Hydrogen configuration	Unshocked	74 ± 4	26 ± 4
	Electrical shocked	35 ± 3	65 ± 3

The influence of electrical shock treatment on the bacterial morphology at a cellular level was examined using SEM at various locations of unshocked and shocked biofilm pre-grown on membrane (Figures 3c, d). Compared to unshocked bacterial cells (Figure 3c), no modification or defects on bacterial cell membranes were observed at this magnitude of scans after the electrical shock (Figure 3d). However, CLSM results revealed that the electric treatment contributed to inactivate 68% of bacteria (Figure 3b, Table 1). Therefore, it can be inferred that the killing of bacteria was carried out but no perceptible modification in the structure of bacterial cells was observed at the employed scan level. In agreement with other studies, neither chlorine disinfection nor electrical shock results in damage to the bacterial membrane cells [63-65]. Hence, the electrical treatment solely causes dysfunction of bacterial cells without inducing any bacterial morphology alteration.

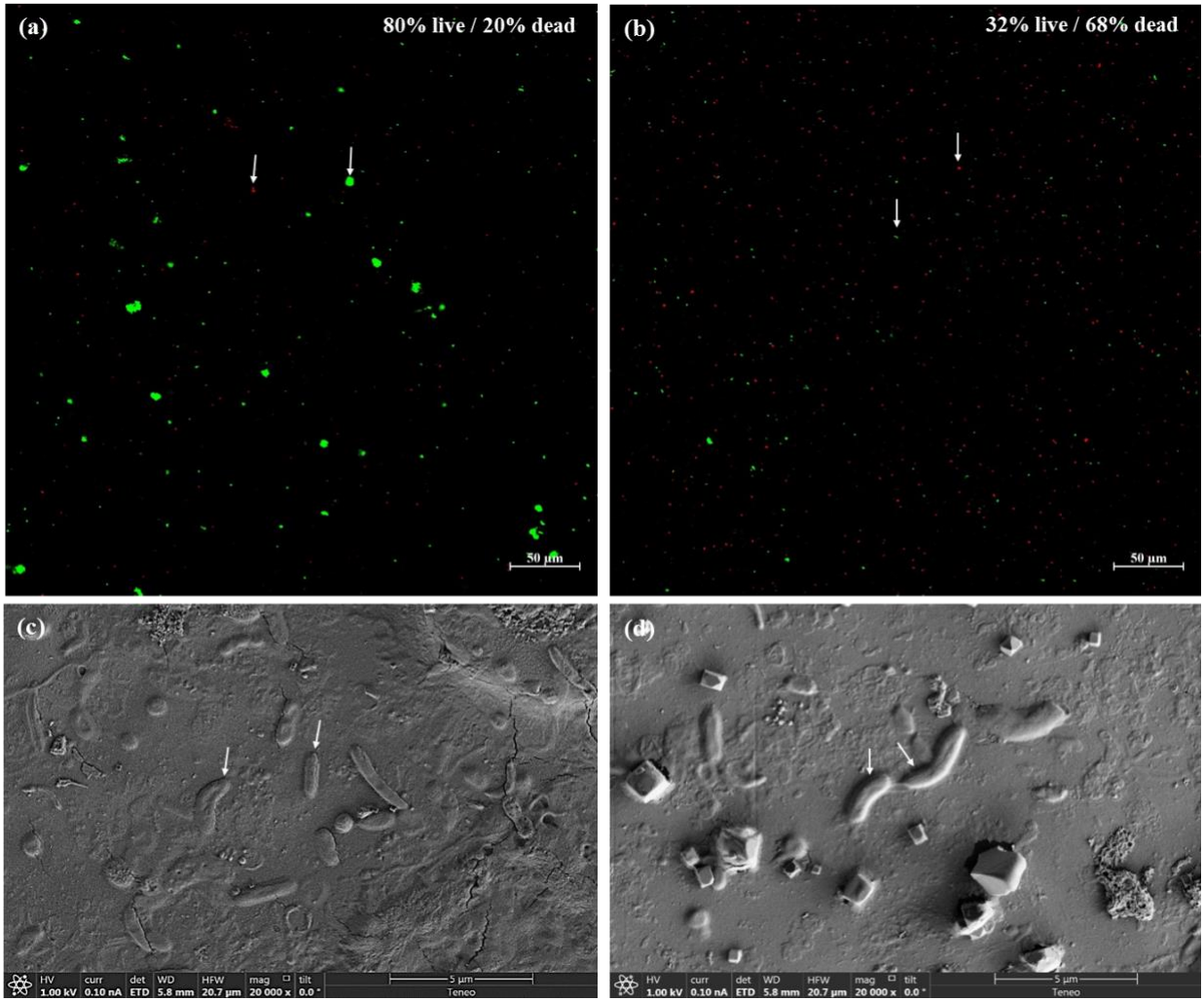

Figure 3. Confocal laser scanning microscopy (a, b) and scanning electron microscopy images (c, d) of unshocked (a, c) and electrically shocked (b, d) bacterial cells of biofouling formed in case of chlorine configuration. The white arrows in the images show the bacterial cells, and the green and red colors in (a, b) represent the live and dead cells, respectively. For electrically treated biofouling samples (b, d), the amounts of free and total chlorine generated are 7 mg/L and 14 mg/L, respectively. The scale bars are 50 µm for (a,b) and 5 µm for (c,d).

3.1.3. In-situ biomass characterization through OCT imaging

The impact of applied DC on the biofilm removal from the membrane surface was *in-situ* investigated within the flow cell unit by OCT imaging. 3D images of the biofilm pre-grown on the membrane surface were visualized and analyzed with high resolution scans at various stages of

treatment as depicted in Figure 4: (a) unshocked at U_0 = 0.073 m/s, (b) unshocked and flushed at U_0 = 0.365 m/s for 30 s and (c) electrically shocked at U_0 = 0.073 m/s (I = 124 mA, t = 90 s) followed by flushing at U_0 = 0.365 m/s for 30 s.

OCT scans revealed that the untreated biofilm, which was initially developed at a linear velocity of 0.073 m/s, displayed dense biomass with a volume estimated of 0.0098 mm^3 (Figure 4a). To check the strong attachment of biofilm to the membrane and spacer surfaces, the velocity was increased to 0.365 m/s resulting in a dislodge of minor biomass volume under high-velocity conditions. Then, the resulting biomass volume decreased slightly to reach 0.0084 mm^3 (Figure 4b). However, when the biofilm was placed under DC (124 mA for 90 s at U_0 = 0.073 m/s) in the presence of chlorine crossing over the biofilm (7 mg/L of free chlorine, Figure 2a) followed by flushing at high velocity (U_0 = 0.365 m/s), the biofouled material was almost completely detached from the membrane surface resulting in a very-small remaining biomass volume of 0.0001 mm^3 on the membrane, as shown in Figure 4c. The percentage of removed biomass reached 99% compared to the biomass volume of untreated sample. Furthermore, photography images were taken for this experiment on the top of the filtration system (spacer/membrane) before and after the electrical shock and presented as insets in Figure 4. They exhibited that the major biomass was successfully swept away from the membrane surface as well as from the spacer after the application of electrical shock. The average biomass cleaning obtained through triplicated experiments was found to be 90%±13% for chlorine configuration.

These findings confirmed the potential of this novel approach to eliminate the biofouling developed on UF membrane. In this chlorine configuration, the pre-grown biofilm is exposed to several factors resulted from the electrolysis process occurred during the application of electrical shock: (i) production of chlorine compounds (HOCl/ ClO^-), (ii) formation of NaOH in the medium and (iii) hydrodynamic shear provided by gas microbubbles flowing over the biofilm. One or more of these factors generated around the biofilm environment caused the cleaning ability of the proposed technique. Therefore, we aimed in the next section to segregate the chlorine effect by switching the electrode-producing chlorine to the outlet side of the flow cell (hydrogen configuration). As a result, the interaction of chlorine compounds with the pre-grown biofilm was eliminated. Consequently, the investigation of hydrogen configuration effectiveness has two targets: (i) exploring if other factors of electrolysis process than chlorine are involved in the bacterial inactivation and biofouling removal, (ii) examining the consistency of technique potential

in absence of chlorine for a universal filtration application as it is known that the presence of chlorine without control could damage other types of membranes such as reverse osmosis (RO) based on aromatic polyamide membranes [66, 67].

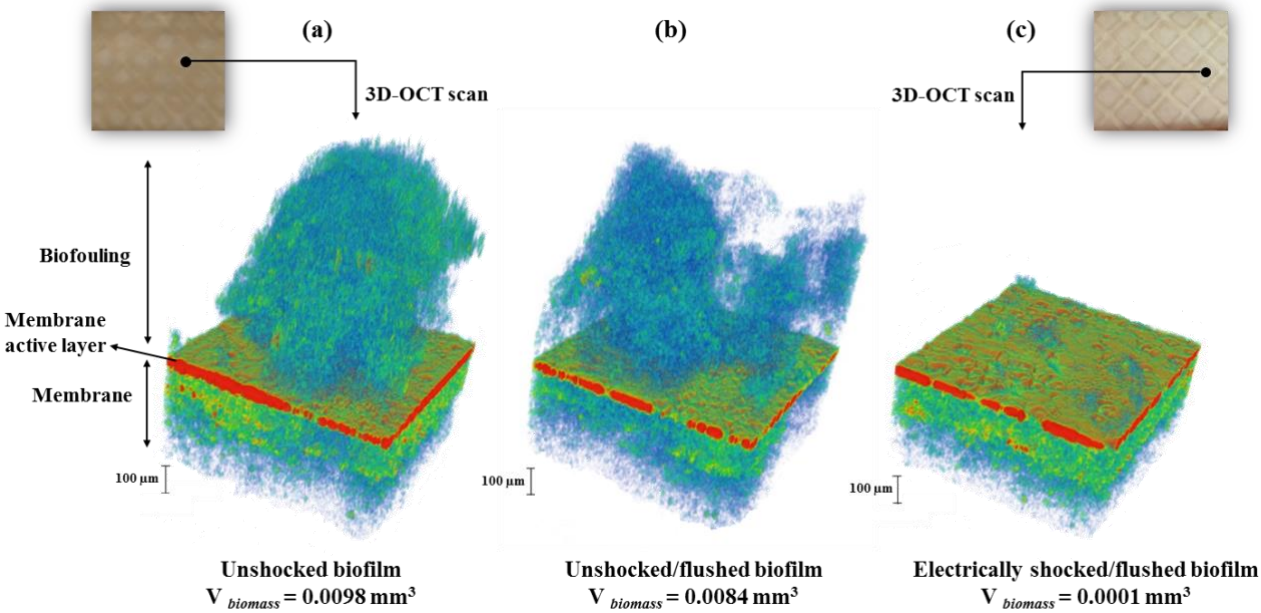

Figure 4. Biofilm removal assessed by 3D-OCT images of biofouling/membrane as a function of various treatment steps acquired in case of chlorine configuration: unshocked at U_0 = 0.073 m/s (a), unshocked and flushed at U_0 = 0.365 m/s for 30 s (b), and electrically shocked (124 mA for 90 s at U_0 = 0.073 m/s, pH $_{\text{treated medium}}$ = 8.4) then flushed at U_0 = 0.365 m/s for 30 s (c). The scale bar (100 µm) corresponds to Y-axis direction. The photography insets represent the filtration system in case of (a) and (c), and the black dots indicate the OCT scanned area location. The color spectrum visualized in the biofouling/membrane structure is related to the light reflection intensity of each material. Consequently, the membrane active layer and fluid flowing through the biofouling/membrane are visualized in a similar color (orange) due to their close reflection intensity. Likewise, the membrane support layer and biomass material appear in the shade of blue to green colors.

3.2. Hydrogen configuration

As in chlorine configuration, CLSM and OCT imaging were achieved for unshocked and electrically shocked pre-grown biofilm in case of hydrogen configuration, where no chlorine could

be involved to influence the biofilm. The results were displayed in Figure 5 and the average viability percentages of live/dead cells were summarized in Table 1. CLSM characterization revealed that 65% of bacterial cells were inactivated when an electrical shock was applied in case of hydrogen configuration (Figure 5b, Table 1). The estimated percentage of dead cells was slightly lower than this obtained in presence of chlorine (68% of dead cells in chlorine configuration, Figure 3b, Table 1). It exposed a significantly higher percentage when compared to this obtained in case of unshocked biofilm (26% of dead cells, Figure 5a, Table 1). These results confirmed that the killing of bacteria was carried out even though the chlorine species were absent from the biofilm environment. In the present configuration, NaOH is only present in the medium. This caustic base, which is further known as a disinfectant agent, has the ability to interact with the biofilm and inactivate the bacteria [61, 62]. It is important to highlight here that the measured pH of the solution that was collected externally from the flow cell was determined to be 8.4 under the applied electrical shock conditions. However, as the feed solution was continuously flowing over the biofilm, the collected solution would undergo slight dilution. Consequently, the local pH between the electrodes (where biofilm resides) would be higher [68, 69] with a higher concentration of NaOH present during electrolysis process. Although it is highly desirable to measure pH online locally near the electrode, owing to experimental complexity and small channel height, the measurement of pH was only achievable offsite, as depicted in Figure 1. Thus, potential bacterial inactivation for this configuration is primarily associated with local pH change occurring between the electrodes. However, slight less bacterial inactivation is observed in this case compared to chlorine configuration, where the presence of additional chlorine compounds (HOCl/ ClO^-) led to a supplementary bactericidal action on microorganisms in agreement with Hülsheger and Niemann [36]. These authors observed a slight increase of surviving cell number when microbial suspensions containing other than sodium chloride electrolytes (phosphate or sulfate) were electrically pulsed at high voltage.

Moreover, as in chlorine configuration, OCT images realized at various steps of treatment (Figures 5c-e) demonstrated that the untreated biomass volume reduced slightly after flushing at high velocity (U_0 = 0.365 m/s) for 30 s ($V_{biomass}$ = 0.0037 mm^3, Figure 5d) when compared to the initial pre-grown biomass volume ($V_{biomass}$ = 0.0040 mm^3, Figure 5c). However, this biomass volume significantly decreased when the electrical shock was applied (124 mA for 90 s at U_0 = 0.073 m/s) followed by flushing at high linear velocity (U_0 = 0.365 m/s) for 30 s ($V_{biomass}$ = 0.0009

405 mm^3, Figure 5e). Therefore, 77% of initial pre-grown biomass were detached from the membrane
406 surface as a result of electrical treatment in the absence of chlorine. The average biomass cleaning
407 obtained through triplicated experiments was found to be 71%±14% for hydrogen configuration.
408

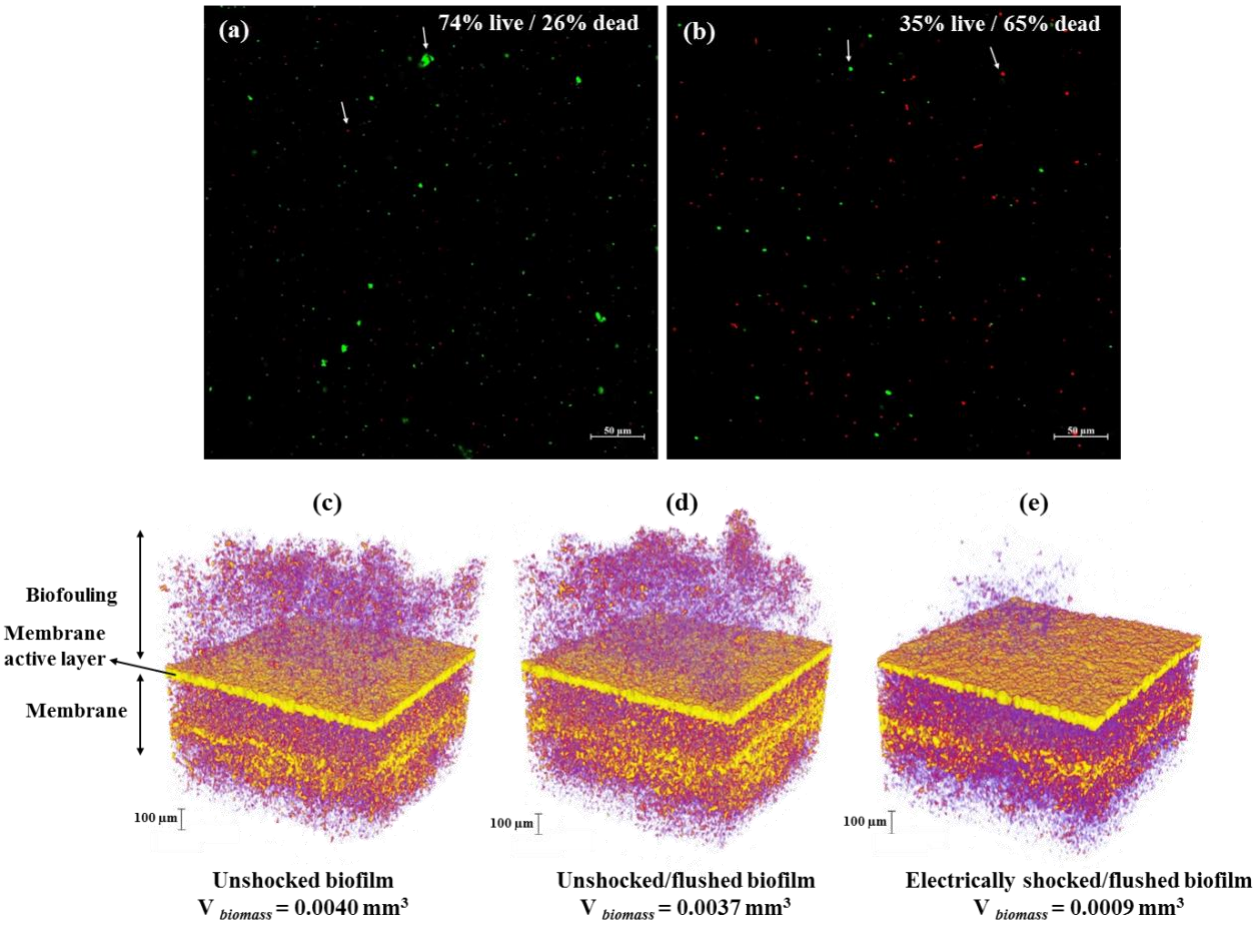

409

410 Figure 5. Live/dead cells (green and red colors, respectively) of unshocked (a) and electrically
411 shocked bacterial cells (b) characterized by confocal laser scanning microscopy, and biofilm
412 removal assessed by 3D-OCT images of biofouling/membrane as a function of various treatment
413 steps acquired in case of hydrogen configuration: unshocked at U_0 = 0.073 m/s (c), unshocked and
414 flushed at U_0 = 0.365 m/s for 30 s (d), and electrically shocked (124 mA for 90 s at U_0 = 0.073
415 m/s, pH $_{\text{treated medium}}$ = 8.4) then flushed at U_0 = 0.365 m/s for 30 s (e). The scale bar (100 µm)
416 corresponds to Y-axis direction. For (c-e), as explained in Figure 4, due to close reflection
417 intensities, the membrane active layer and fluid flowing appear in a similar color (yellow), while
418 the membrane support layer and biomass material are visualized in purple color.

Indeed, it is relevant to emphasize here that although for both configurations (chlorine or hydrogen) the biofilm was pre-grown on membrane surface for 10 days under the same experimental conditions, a different thickness of biofilm was observed for the two configurations (Figures 4a and 5c). This is primarily associated with the heterogeneous nature of biofilm growth. As OCT probe was fixed for both configurations at the same location, a different volume of biofilm was observed in each configuration. However, statistical averaging of biofilm thickness at varied locations in the flow cell reveals about 228±13 μm as average biofilm thickness for both configurations, suggesting that experimental conditions were well controlled for biofilm growth. The percentage of biofilm removal achieved after electrical shock and flushing was determined relative to its corresponding biomass volume initially developed on the membrane surface (as mentioned in Section 2.3). Consequently, the deficiency of maintaining a constant initial biofilm volume for both cases does not influence the results of subsequent treatment stages. Thus, although the cleaning potential in hydrogen configuration was not as effective as seen in case of chlorine configuration where almost the entire biofilm was removed from the membrane surface (Figure 4c), the high efficiency of the proposed technique to sweep away the biofouling was successfully confirmed.

3.3. Mechanism of biofilm removal using direct electrical current

The present work successfully demonstrates that a direct electrical current applied across the flow cell through Pt electrodes immersed in seawater can effectively remove the pre-grown biofilm from membrane surface. Several competing factors are potentially responsible for this efficient biofilm removal. To understand these factors, the electrolysis process carried out due to DC application inside the flow-cell needs to be highlighted. When a voltage potential is applied through Pt electrodes immersed in seawater, the primary ions presented in the medium (Na^+/Cl^- and H^+/OH^-) are attracted to oppositely charged electrodes. Consequently, the loss and gain of electrons (achieved by Cl^- and H^+, respectively) at each electrode due to redox reactions (Eqs. 1-5) complete the external electrical circuit. Thus, no flow of electrons through the water or biofilm takes place as neither the membrane nor the spacer used has an electro-conductive property. Moreover, the electrodes were not located in direct contact with the membrane/spacer. Therefore, under the given scenario, no direct impact of the electrical field can be envisaged on the biofilm removal for both tested configurations (chlorine or hydrogen). Only electrochemical reactions

occurred at electrodes that generate chemical/physical products, could potentially aid in uprooting the existing pre-grown biofilm from the membrane surface. Under given experimental conditions, only three potential products can interact with the biofilm after electrolysis: (i) chlorine species $HOCl/ClO^-$, (ii) NaOH base, and/or (iii) gas microbubbles (chlorine or hydrogen) flowing over the biofilm.

Noticeably, the chemical interaction of chlorine species ($HOCl/ClO^-$) with the biofilm is only possible in the chlorine configuration case when the electrode-producing chlorine is kept at the inlet. A higher percentage of biofilm cleaning is achieved for the chlorine configuration compared to hydrogen configuration where chlorine species exit out of the flow cell without affecting the biofilm. Hence, it is inevitably to infer that the presence of chlorine is not common as well as the major factor that aids in biofilm removal. Therefore, the fundamental mechanism of biofilm removal can be primarily attributed to NaOH formation (local pH change) and/or the hydrodynamic shear created by flowing gas microbubbles in both configurations.

These proposed hypotheses are tested by performing additional individual experiments (experimental protocol described in Section S2 of Supplementary material). NaOH, NaOCl, and gas microbubbles are systematically isolated to experimentally investigate the cleaning efficacy of each component. The relative cleaning performance for each investigated case is shown in Figure 6. It can be concluded that the effect of chlorine was negligible. Simultaneously, NaOH influence and gas microbubble force were found to aid quite a bit in biofilm removal. Averages of 34% and 67% of biomass volume removal were independently achieved for NaOH and microbubbles, respectively. The highest potential of biomass uprooting was then attributed to the mechanical shear of gas microbubbles generated through electrolysis.

Based on these findings, it can be affirmatively confirmed that NaOH and microbubble interactions with biofilm are primarily responsible for the cleaning action. Previous studies [37, 46, 70] reported that the introduction of a dilute base solution caused deformation in the biofilm structure and could also aid in weakening its mechanical stability resulting in its detachment from the membrane surface. In our study, an increase in local pH was monitored due to the formation of alkali (NaOH) over the pre-grown biofilm when an electric current was applied. Biofilms are primarily composed of polymeric content (EPS), which ensures the intercellular cooperation within the matrix and provides the mechanical stability to the biofilm [46, 71]. The generation of NaOH led to hydrolyze the polysaccharide matrix of the biofilm (EPS) [46, 71]. As EPS acts as a

glue between the biofilm and the membrane/spacer [46, 71], any deformation of its structure induces the deterioration of the entire biofilm resulting in its removal from the membrane. Besides, gas microbubbles (chlorine or hydrogen) were simultaneously generated through electrochemical reactions and flow over and around the biofilm. These microbubbles also exert a shear force on the microbial community resulting in further weakening its attached biomass [46, 72].

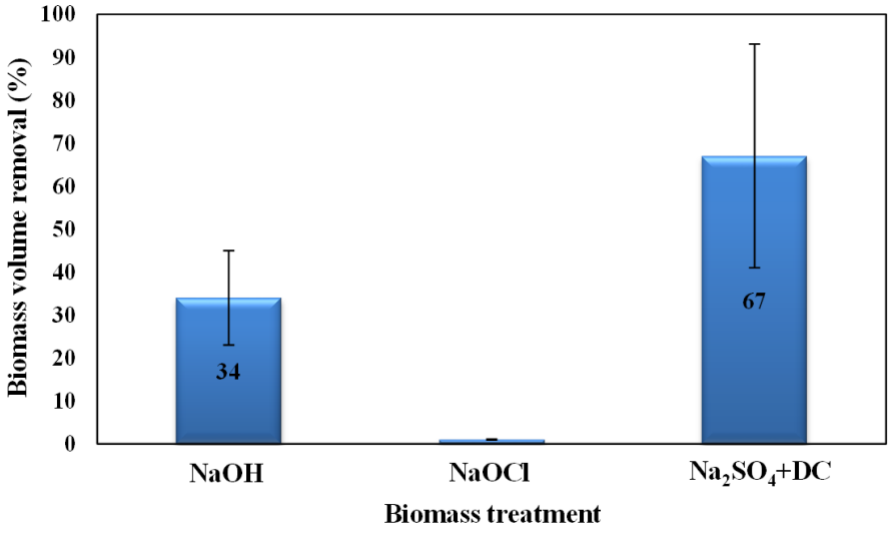

Figure 6. Percentage of biomass volume removal at various applied treatments. The percentage of biomass removal was calculated based on initial and final biomass volumes on membrane surface determined by using 3D-OCT characterization (as achieved in Figures 4 and 5) for each treatment case.

4. Perspectives

The outcomes of this study suggest that the application of electrical shock to the biofilm aids in cleaning the membrane surface effectively in a very short time scale. Although the biofilm had high resistance against the fluid shear force exerted by increasing the linear flow velocity (Figures 4b and 5d), it appeared that biofilm bonds or stickiness were compromised under the influence of electrolysis process induced by an electric current application and the biofilm removal from the membrane surface was effectively achieved. This cleaning method provides an attractive and very straightforward way to effectively sweep away the biofouling from UF membrane systems. The proposed technique also potentially appears to be energy efficient compared to exiting Clean-In-Place (CIP) technologies used in commercial plants. From the presented results, for a single

electrical shock process the amount of electrical power consumed should be around P = 7.68 Watt (P = E*I, where E = 62 V and I =124 mA). In general, CIP pumps and compressors consume much higher energy than the proposed method. In addition, small homogeneous gas bubbles generated through this technique were found not to coalesce, and passed easily through the channel, avoiding one of the major challenges in aeration based cleaning technology [73-75]. However, the direct application of this technology on real filtration modules, which are few meters in length, may require some subtle changes to achieve a high cleaning potential. For instance, the use of spacer type metal electrodes at inlet and outlet can be embedded in each filtration channel, while having the regular plastic spacer in between the electrodes could serve as one option. For this design, a greater length of metallic conductive spacers relative to plastic spacers is encouraged to ensure a greater cleaning efficiency. Another alternative would be to insert multiple Pt wire electrodes as electrodes connected in series across the length of the module at a specified distance. All these Pt wires could be electrically energized systematically to considerably promote the electrolysis process across the module.

Even though this approach might require a higher voltage extent in real filtration modules, DC will be applied intermittently and only for a short shock time, which limits the energy requirement. Contrary to CIP technique, once the electrodes are installed in the filtration, neither additional equipment nor chemical products will be needed to integrate the system for proceeding the biofilm removal. Moreover, this technique is *in-situ* applied in two consecutive steps (electric shock and flush) without any heating process (as encountered in other techniques). All these aforementioned benefits help to minimize the energy consumption of filtration systems. Compared to the traditional CIP methods, we foresee easier installation, handling, and lower energy consumption as key points for the adaption of this technology to commercial water treatment plants.

Intermittent electrical shocks regularly applied from the onset of the filtration process might mitigate or even delay the growth of biofilm. Therefore, further studies are aimed to be realized to deeply demonstrate the potential of this approach in preventing/controlling the biofouling growth in UF membranes. In the nearest future, research studies are planned to be performed to extend this approach in other filtration systems (RO, NF) in a controlled manner.

5. Conclusions

Removal of pre-grown biofilm from UF membrane surface by using direct electric current is successfully investigated in this study. The amount of chlorine generated via the electrochemical reactions was found to be *in-situ* controlled by varying several operating parameters. A near-complete cleaning potential (99%) associated with high bacterial inactivation (68%) was achieved when the electrode-producing chlorine was placed at the flow cell inlet. However, placing this electrode at the outlet side led to a slightly lower biofilm removal (77%) and bacterial inactivation (65%). The biofilm removal mechanism was mainly attributed to the synergic effect of gas microbubbles and the caustic agent (NaOH) which were simultaneously generated during electrolysis process.

Author Contributions

The manuscript was written through contributions of all authors. All authors have given approval to the final version of the manuscript.

Acknowledgment

The research reported in this paper was supported by King Abdullah University of Science and Technology (KAUST), Saudi Arabia. The authors extend their gratitude to the Water Desalination and Reuse Center (WDRC) staff for their continuous support. Imaging and Characterization Lab (ICL) staff is also highly acknowledged for their assistance and support in this project.

References

[1] J. Wingender, T.R. Neu, H.-C. Flemming, Microbial extracellular polymeric substances: Characterization, structure and function, Springer, (1999).

[2] J. Mansouri, S. Harrissonbc, V. Chen, Strategies for controlling biofouling in membrane filtration systems: challenges and opportunities, J. Mater. Chem., 20 (2010) 4567-4586.

[3] T. Nguyen, F. Roddick, L. Fan, Biofouling of water treatment membranes: A review of the underlying causes, monitoring techniques and control measures, Membranes, 2 (2012) 804.

[4] G. Goldman, J. Starosvetsky, R. Armon, Inhibition of biofilm formation on UF membrane by use of specific bacteriophages, J. Membr. Sci., 342 (2009) 145-152.

[5] S. Kappachery, D. Paul, J. Yoon, J.H. Kweon, Vanillin, a potential agent to prevent biofouling of reverse osmosis membrane, Biofouling, 26 (2010) 667-672.
[6] S. Kim, S. Lee, S. Hong, Y. Oh, M. Seoul, J. Kweon, T. Kim, Biofouling of reverse osmosis membranes: Microbial quorum sensing and fouling propensity, Desalination, 247 (2009) 303-315.
[7] N. Barraud, M.V. Storey, Z.P. Moore, J.S. Webb, S.A. Rice, S. Kjelleberg, Nitric oxide-mediated dispersal in single- and multi-species biofilms of clinically and industrially relevant microorganisms, Microb. Biotechnol., 2 (2009) 370-378.
[8] M. Wilf, S. Alt, Application of low fouling RO membrane elements for reclamation of municipal wastewater, Desalination, 132 (2000) 11-19.
[9] J.S. Vrouwenvelder, F. Beyer, K. Dahmani, N. Hasan, G. Galjaard, J.C. Kruithof, M.C.M. Van Loosdrecht, Phosphate limitation to control biofouling, Water Res., 44 (2010) 3454-3466.
[10] T.M. Missimer, N. Ghaffour, A.H.A. Dehwah, R. Rachman, R.G. Maliva, G. Amy, Subsurface intakes for seawater reverse osmosis facilities: Capacity limitation, water quality improvement, and economics, Desalination, 322 (2013) 37-51.
[11] C.X. Liu, D.R. Zhang, Y. He, X.S. Zhao, R. Bai, Modification of membrane surface for anti-biofouling performance: Effect of anti-adhesion and anti-bacteria approaches, J. Membr. Sci., 346 (2010) 121-130.
[12] Z. Liu, Y. Hu, Sustainable antibiofouling properties of thin film composite forward osmosis membrane with rechargeable silver nanoparticles loading, ACS Appl. Mater. Interfaces, 8 (2016) 21666-21673.
[13] A.K. Singh, S. Prakash, V. Kulshrestha, V.K. Shahi, Cross-linked hybrid nanofiltration membrane with antibiofouling properties and self-assembled layered morphology, ACS Appl. Mater. Interfaces, 4 (2012) 1683-1692.
[14] L. Yao, C. He, S. Chen, W. Zhao, Y. Xie, S. Sun, S. Nie, C. Zhao, Codeposition of polydopamine and zwitterionic polymer on membrane surface with enhanced stability and antibiofouling property, Langmuir, 35 (2018) 1430-1439.
[15] P. Gunawan, C. Guan, X. Song, Q. Zhang, S.S.J. Leong, C. Tang, Y. Chen, M.B. Chan-Park, M.W. Chang, K. Wang, R. Xu, Hollow fiber membrane decorated with Ag/MWNTs: Toward effective water disinfection and biofouling control, ACS Nano, 5 (2011) 10033-10040.

[16] X. Lu, X. Feng, X. Zhang, M.N. Chukwu, C.O. Osuji, M. Elimelech, Fabrication of a desalination membrane with enhanced microbial resistance through vertical alignment of graphene oxide, Environ. Sci. Technol. Lett., 5 (2018) 614-620.
[17] S. Kerdi, A. Qamar, J.S. Vrouwenvelder, N. Ghaffour, Fouling resilient perforated feed spacers for membrane filtration, Water Res., 140 (2018) 211-219.
[18] N. Ghaffour, A. Qamar, Fouling resistant membrane spacers, Patent publication N°. WO 2017/175137 A1 (2017).
[19] S.M. Ali, A. Qamar, S. Kerdi, S. Phuntsho, J.S. Vrouwenvelder, N. Ghaffour, H.K. Shon, Energy efficient 3D printed column type feed spacer for membrane filtration, Water Res., 164 (2019) 114961.
[20] S. Kerdi, A. Qamar, A. Alpatova, J.S. Vrouwenvelder, N. Ghaffour, Membrane filtration performance enhancement and biofouling mitigation using symmetric spacers with helical filaments, Desalination, 484 (2020) 114454.
[21] N. Ghaffour, A. Qamar, Membrane fouling quantification by specific cake resistance and flux enhancement using helical cleaners, Sep. Purif. Technol., 239 (2020) 116587.
[22] A. Qamar, S. Bucs, C. Picioreanu, J. Vrouwenvelder, N. Ghaffour, Hydrodynamic flow transition dynamics in a spacer filled filtration channel using direct numerical simulation, J. Membr. Sci., 590 (2019) 117264.
[23] N. Hilal, O.O. Ogunbiyi, N.J. Miles, R. Nigmatullin, Methods employed for control of fouling in MF and UF membranes: A comprehensive review, Sep. Sci. Technol., 40 (2005) 1957-2005.
[24] C. Psoch, S. Schiewer, Resistance analysis for enhanced wastewater membrane filtration, J. Membr. Sci., 280 (2006) 284-297.
[25] A. Alpatova, A. Qamar, M. Al-Ghamdi, J. Lee, N. Ghaffour, Effective membrane backwash with carbon dioxide under severe fouling and operation conditions, J. Membr. Sci., 611 (2020) 118290.
[26] A. Lo″rincz, Ultrasonic cellular disruption of Yeast in water-based suspensions, Biosyst. Eng., 89 (2004) 297-308.
[27] A. Qamar, L. Fortunato, T. Leiknes, Acoustically excited encapsulated microbubbles and mitigation of biofouling, Patent publication N°. WO 2017/145118 A1 (2017).
[28] A. Qamar, R. Samtaney, J.L. Bull, Dynamics of micro-bubble sonication inside a phantom vessel, Appl. Phys. Lett., 102 (2013) 013702.

[29] S. Lattemann, T. Höpner, Environmental impact and impact assessment of seawater desalination, Desalination, 220 (2008) 1-15.
[30] N.M. Farhat, E. Loubineaud, E.I.E.C. Prest, J. El-Chakhtoura, C. Salles, S.S. Bucs, J. Trampé, W.B.P. Van den Broek, J.M.C. Van Agtmaal, M.C.M. Van Loosdrecht, J.C. Kruithof, J.S. Vrouwenvelder, Application of monochloramine for wastewater reuse: Effect on biostability during transport and biofouling in RO membranes, J. Membr. Sci., 551 (2018) 243-253.
[31] J.C.-T. Lin, D.-J. Lee, C. Huang, Membrane fouling mitigation: Membrane cleaning, J. Sep. Sci., 45 (2010) 858-872.
[32] E. Zondervan, B. Roffel, Evaluation of different cleaning agents used for cleaning ultra filtration membranes fouled by surface water, J. Membr. Sci., 304 (2007) 40-49.
[33] J.S. Baker, L.Y. Dudley, Biofouling in membrane systems - A review, Desalination, 118 (1998) 81-89.
[34] A. Kraft, Electrochemical water disinfection: A short review, Platin. Met. Rev., 52 (2008) 177-185.
[35] J.-C. Park, M.S. Lee, D.H. Lee, B.J. Park, D.-W. Han, M. Uzawa, K. Takatori, Inactivation of bacteria in seawater by low-amperage electric current, Appl. Environ. Microbiol., 69 (2003) 2405-2408.
[36] H. Hülsheger, E.-G. Niemann, Lethal effects of high-voltage pulses on E. coli K12, Radiat. Environ. Biophys., 18 (1980) 281-288.
[37] G.M. Ayoub, R. Zayyat, N. Naji, Electric current induced bacterial inactivation in seawater: Effects of various operating conditions, Int. J. Environ. Sci. Technol., 16 (2019) 4749-4760.
[38] Y. Birbir, N. Dolek, M. Birbir, Effect of a combined treatment using both direct and alternating electric currents on hide bacteria in hide-soak liquor, J. Electrostat., 71 (2013) 898-904.
[39] J.-C. Park, M.S. Lee, D.-W. Han, D.H. Lee, B.J. Park, I.-S. Lee, M. Uzawa, M. Aihara, K. Takatori, Inactivation of Vibrio parahaemolyticus in effluent seawater by alternating-current treatment, Appl. Environ. Microbiol., 70 (2004) 1833.
[40] P.C. Wouters, N. Dutreux, J.P.P.M. Smelt, H.L.M. Lelieveld, Effects of pulsed electric fields on inactivation kinetics of Listeria innocua, Appl. Environ. Microbiol., 65 (1999) 5364-5371.
[41] H. Bergmann, T. Iourtchouk, K. Schöps, K. Bouzek, New UV irradiation and direct electrolysis - promising methods for water disinfection, Chem. Eng. J., 85 (2002) 111-117.

[42] G. Brunner, E. Okoro, Reduction of membrane fouling by means of an electric field during ultrafiltration of protein solutions, Ber. Bunsenges. Phys. Chem., 93 (1989) 1026-1032.
[43] C.C. Tarazaga, M.E. Campderrós, A.P. Padilla, Physical cleaning by means of electric field in the ultrafiltration of a biological solution, J. Membr. Sci., 278 (2006) 219-224.
[44] C.F. De Lannoy, D. Jassby, K. Gloe, A.D. Gordon, M.R. Wiesner, Aquatic biofouling prevention by electrically charged nanocomposite polymer thin film membranes, Environ. Sci. Technol., 47 (2013) 2760-2768.
[45] Y. Baek, H. Yoon, S. Shim, J. Choi, J. Yoon, Electroconductive feed spacer as a tool for biofouling control in a membrane system for water treatment, Environ. Sci. Technol. Lett., 1 (2014) 179-184.
[46] C. Rabinovitch, P.S. Stewart, Removal and inactivation of Staphylococcus epidermidis biofilms by electrolysis, Appl. Environ. Microbiol., 72 (2006) 6364-6366.
[47] A.J. van der Borden, H. van der Werf, H.C. van der Mei, H.J. Busscher, Electric current-induced detachment of Staphylococcus epidermidis biofilms from surgical stainless steel, Appl. Environ. Microbiol., 70 (2004) 6871-6874.
[48] M. Aslam, R. Ahmad, J. Kim, Recent developments in biofouling control in membrane bioreactors for domestic wastewater treatment, Sep. Purif. Technol., 206 (2018) 297-315.
[49] S.N. Jagannadh, H.S. Muralidhara, Electrokinetics methods to control membrane fouling, Ind. Eng. Chem. Res., 35 (1996) 1133-1140.
[50] P.v. Zumbusch, W. Kulcke, G. Brunner, Use of alternating electrical fields as anti-fouling strategy in ultrafiltration of biological suspensions - Introduction of a new experimental procedure for crossflow filtration, J. Membr. Sci., 142 (1998) 75-86.
[51] A.V. Dudchenko, C. Chen, A. Cardenas, J. Rolf, D. Jassby, Frequency-dependent stability of CNT Joule heaters in ionizable media and desalination processes, Nat. Nanotechnol., 12 (2017) 557-563.
[52] A. Qamar, S. Kerdi, J.S. Vrouwenvelder, N. Ghaffour, Biofouling removal and mitigation using direct electrical shock technology (DEST) in water treatment systems, Patent publication, International application N°. PCT/IB2020/051140 (2020).
[53] S. Kerdi, A. Qamar, A. Alpatova, N. Ghaffour, An *in-situ* technique for the direct structural characterization of biofouling in membrane filtration, J. Membr. Sci., 583 (2019) 81-92.

[54] G.E. Stoner, G.L. Cahen, M. Sachyani, E. Gileadi, The mechanism of low frequency a.c. electrochemical disinfection, J. Electroanal. Chem., 141 (1982) 229-243.
[55] S. Abderrahmane, A. Himour, L. Ponsonnet, Inactivation of E. coli and Pseudomonas aeruginosa by electrochloration under bipolar pulsed polarization, Mater. Sci. Eng. C, 28 (2008) 901-905.
[56] H. Nath, X. Wang, R. Torrens, A. Langdon, A novel perforated electrode flow through cell design for chlorine generation, J. Appl. Electrochem., 41 (2011) 389-395.
[57] J. Jeong, J.Y. Kim, M. Cho, W. Choi, J. Yoon, Inactivation of Escherichia Coli in the electrochemical disinfection process using a Pt anode, Chemosphere, 67 (2007) 652-659.
[58] X.Y. Li, H.F. Diao, F.X.J. Fan, J.D. Gu, F. Ding, A.S.F. Tong, Electrochemical wastewater disinfection: Identification of its principal germicidal actions, J. Environ. Eng., 130 (2004) 1217-1221.
[59] S.-V. Len, Y.-C. Hung, M. Erickson, C. Kim, Ultraviolet spectrophotometric characterization and bactericidal properties of electrolyzed oxidizing water as influenced by amperage and pH, J. Food Prot., 63 (2000) 1534-1537.
[60] T.J. Battin, L.A. Kaplan, J.D. Newbold, X. Cheng, C. Hansen, Effects of current velocity on the nascent architecture of stream microbial biofilms, Appl. Environ. Microbiol., 69 (2003) 5443-5452.
[61] P.G. Mazzola, A.M.S. Martins, T.C.V. Penna, Chemical resistance of the gram-negative bacteria to different sanitizers in a water purification system, BMC Infect. Dis., 6 (2006) 131.
[62] M. Corcoran, D. Morris, N. De Lappe, J. O'Connor, P. Lalor, P. Dockery, M. Cormican, Commonly used disinfectants fail to eradicate Salmonella enterica biofilms from food contact surface materials, Appl. Environ. Microbiol., 80 (2014) 1507-1514.
[63] H.F. Diao, X.Y. Li, J.D. Gu, H.C. Shi, Z.M. Xie, Electron microscopic investigation of the bactericidal action of electrochemical disinfection in comparison with chlorination, ozonation and Fenton reaction, Process Biochem., 39 (2004) 1421-1426.
[64] W.A. Hamilton, A.J.H. Sale, Effects of high electric fields on microorganisms: II. Mechanism of action of the lethal effect, Biochim. Biophys. Acta, 148 (1967) 789-800.
[65] G. White, Handbook of chlorination and alternative disinfectants, 4th ed. New York: Wiley (1999) p. 57-94.

[66] J.M. Gohil, A.K. Suresh, Chlorine attack on reverse osmosis membranes: Mechanisms and mitigation strategies, J. Membr. Sci., 541 (2017) 108-126.
[67] D.H. Shin, N. Kim, Y.T. Lee, Modification to the polyamide TFC RO membranes for improvement of chlorine-resistance, J. Membr. Sci., 376 (2011) 302-311.
[68] K. Murase, T. Honda, T. Hirato, Y. Awakura, Measurement of pH in the vicinity of a cathode during the chloride electrowinning of nickel, Metal. Mater. Trans. B 29 (1998) 1193-1198.
[69] C.-Y. Chan, K.H. Khoo, T.K. Lim, A.T. Kuhn, Determination of pH changes in the near-electrode solution layer at a nickel cathode during electrolysis of NaCl solutions, Surface Technology, 15 (1982) 383-394.
[70] J.B. Xavier, C. Picioreanu, S.A. Rani, M.C.M. van Loosdrecht, P.S. Stewart, Biofilm-control strategies based on enzymic disruption of the extracellular polymeric substance matrix - a modelling study, Microbiology, 151 (2005) 3817-3832.
[71] K. Antoniou, J.F. Frank, Removal of Pseudomonas putida biofilm and associated extracellular polymeric substances from stainless steel by alkali cleaning, J. Food Prot. , 68 (2005) 277-281.
[72] M.A. Al-Ghamdi, A. Alhadidi, N. Ghaffour, Membrane backwash cleaning using CO2 nucleation, Water Res., 165 (2019) 114985.
[73] S. Elmaleh, N. Ghaffor, Upgrading oil refinery effluents by cross-flow filtration, Water Science and Technology, 34 (1996) 231-238.
[74] I.S. Ngene, R.G.H. Lammertink, A.J.B. Kemperman, W.J.C. van de Ven, L.P. Wessels, M. Wessling, W.G.J. Van der Meer, CO2 Nucleation in Membrane Spacer Channels Remove Biofilms and Fouling Deposits, Ind. Eng. Chem. Res., 49 (2010) 10034-10039.
[75] P. Willems, A.J.B. Kemperman, R.G.H. Lammertink, M. Wessling, M. van Sint Annaland, N.G. Deen, J.A.M. Kuipers, W.G.J. van der Meer, Bubbles in spacers: Direct observation of bubble behavior in spacer filled membrane channels, J. Membr. Sci., 333 (2009) 38-44.